

## Geochemistry of sandstones from the Imphal Valley, Indo-Myanmar Ranges

Salam Ranjeeta Devi

Department of Earth Sciences, Manipur University, Imphal-795003, India

Email: ranjeeta\_27@rediffmail.com

### ABSTRACT

Spheroidal weathered siliciclastic rocks of the Imphal Valley, Indo-Myanmar Ranges were studied to determine paleoclimate, paleoweathering and mineral alteration based on the geochemical and mineralogical compositions. The Chemical Index of Alteration (CIA) suggests low-intermediate chemical weathering. Plagioclase Index of Alteration (PIA) value indicates incipient plagioclase alteration. Mineralogical Index of Alteration (MIA) reveals incipient to intermediate mineralogical alteration and the A-CN-K ternary plot of the studied samples suggests a low rate of alteration. The results suggest semi-arid climate, which ranges from warm-arid to warm cool conditions. Geochemistry and mineralogy indicate felsic, mafic and ultramafic compositions for the siliciclastic rocks.

**Keywords:** Spheroidal Weathering, Imphal Valley, Indo-Myanmar Ranges, paleoweathering and mineral alteration, paleoclimate

### INTRODUCTION

An understanding of weathering processes is essential, since these fundamental processes are responsible for the geomorphological evolution of landscapes (Stallard, 1995; Turkington et al., 2005; Brantley et al., 2011; Hall et al., 2012) and environmental planning (Ehlen, 2005). The knowledge on weathering of the siliciclastic rock is useful in designing road, quarries, excavation and in planning for reclamation at surface mines, an idea of the durability of different sedimentary rocks types is desirable. Unlike crystalline rocks, the study of siliciclastic rock weathering is complicated by lateral and vertical variations in lithology which make it difficult to compare weathered material with unweathered rock. Homogeneous rocks like basalts and coarse-grained granite show spheroidal weathering processes during regolith generation. Spheroidal weathering, also termed concentric or onion-skin weathering, is defined as the process where rocks scale off in concentric shells, producing rounded boulder-like forms (Chapman and Greenfield, 1949; Ollier, 1971). When those rocks are well jointed, the corners of a boulder suffer attacks in all directions and, often, there is an abrupt physical change between the unweathered rock and the weathered rock. The combination of chemical and physical processes in spheroidal weathering enhances the weathering rate. Many studies are carried out on spheroidal weathering to discuss mineralogical changes, geochemical processes (Babechuk et al., 2014), landscape evolution (Fletcher et al., 2006; Brantley et al., 2011) or weathering rates calculation (Chabaux et al., 2013).

Geochemistry of major, trace and REEs of the clastic sedimentary rocks are widely used to infer provenance, paleoweathering, mineral composition, depositional environment and paleoclimate conditions and the elemental ratios of these elements signify the source rocks, paleoclimate and paleoweathering

condition (Bhatia, 1983; McLennan et al. 1993; Hernández-Hinojosa et al., 2018; Anaya-Gregorio et al., 2018; Armstrong-Altrin, 2020). The chemical weathering has effect on the geochemistry and mineralogy of sediments (Nesbitt and young, 1982; McLennan, 1993; Bhatia and Crook, 1986; Roser and Korsch, 1986; Sopia et al., 2023). The present study determines paleoclimate, paleoweathering and mineral alteration, as well as geochemical and mineralogical composition of spheroidal weathered sandstones from the Imphal valley, Indo-Myanmar Ranges (IMR). The objective of this study is to infer the weathering and provenance of sandstones from the Imphal valley.

### GEOLOGICAL SETTING

The Imphal valley and its surrounding areas consist of the Disang Group (Late Cretaceous to Eocene), Disang-Barail transition (Late Eocene- Early Oligocene) and Barail Group (Oligocene) with an alluvium deposit (Fig. 1). The Disang Group consists of dark grey splintery shales with silty shale and fine sandstone, sometimes giving rise to rhythmic character. The gradational contact between the Disang and Barail Group runs nearly parallel to the western margin of the Imphal valley and continue northerly towards the Naga Hills and southerly along Mizo-Hills of the Indo-Myanmar Ranges. The Imphal valley is bounded by two prominent thrust faults, the one in the eastern side is the Thoubal Thrust (TT) while the other in the western side is the Churachandpur Mao-Thrust (CMT), which also partly serves as the tectonic contact between the Disang and Barail Groups.

The Disang-Barail transition sequence of the Imphal Valley are characterized by intercalation of thin, flaggy, well cemented siltstone, fine-grained sandstone and sandy or silty shales (Devi, 2021) with

plant impression such as leaf, twigs, bark etc. The Barail Group occupies the western side of the

silt and sand of fluvio-lacustrine origin, covers a wide area of the valley, above the Barail. Stratigraphic Succession of the Imphal Valley of the Indo-Myanmar ranges is given in Table 1.

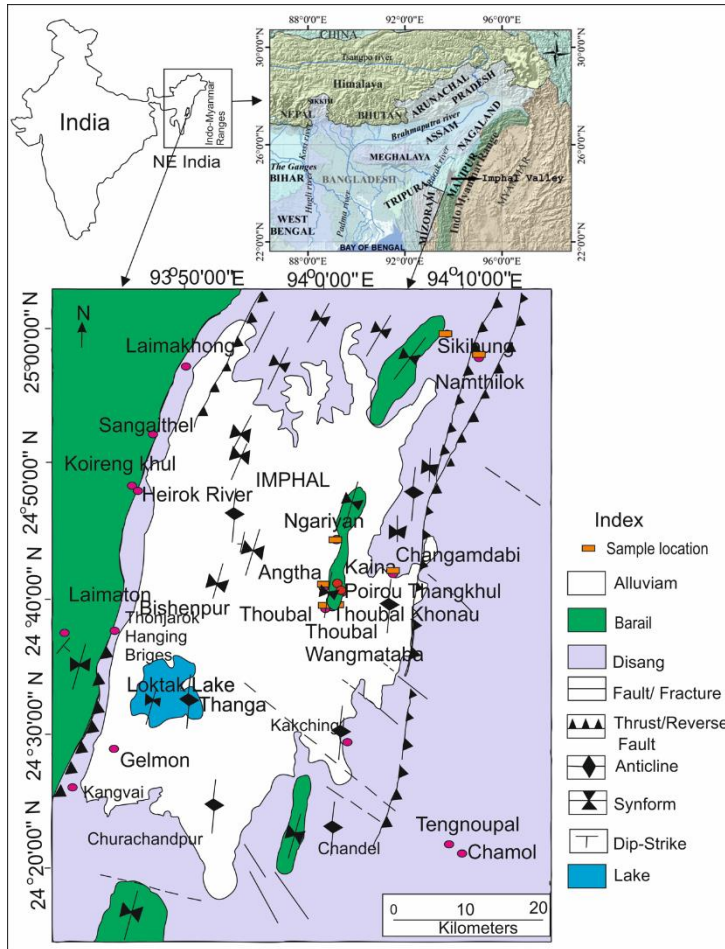


Figure 1. Geological map of the Imphal Valley, Indo-Myanmar Ranges showing the sample locations (modified after Devi, 2022).

**METHODOLOGY**

Sandstone, siltstone and shale samples of spheroidal weathering rocks were collected from the Imphal valley along the road cut and small quarries (Fig. 1). For geochemical analysis, sandstones are thoroughly washed, dried and homogenized in an agate mortar. All concentrations in this work were expressed with reference to dry weight. Samples were powdered by 200 ASTM. Major element concentrations for sample were determined using a RIGAKU ZSX Primus II X-ray Fluorescence Spectrometer system and analyzed in pressed powder briquettes. The accuracy of major elements of each sample was taken in 3 ml savillexR vials, supra pure acid mixture of HF+HNO<sub>3</sub>+HCl in 7:3:1 proportion was added, and heated for about 48 h on a hot plate at a temperature of 110°C with lids closed. The samples were repeatedly treated with HNO<sub>3</sub> + HCl until clear solutions were obtained. The solutions were dried, re-dissolved with 2% HNO<sub>3</sub> and diluted to 50 ml in polypropylene (PP) storage bottles. The stock solution was further diluted to ~7500 times with 2% HNO<sub>3</sub>, and trace and REE concentrations were measured using Inductively Coupled Plasma-Quadrapole Mass Spectrometer (ICPMS, Thermo X-Series) at the Department of Earth Sciences, Pondicherry University. USGS

Table 1. Stratigraphic succession of the Imphal Valley (Soibam, 1997)		
Group	Lithology	Age
Alluviums	Dark grey to black clay, silt and sand deposits of fluvial-lacustrine origin. Flood plain deposits of the rivers and streams. Clay, sand, gravel and boulder deposits of the foothills and old river terraces. Possibly including lower deposits of the Imphal Valley.	(Quaternary: Holocene to Pleistocene (?) Older)
<b>-----Stratigraphic Break-----</b>		
Barails	Shale, sandy shale, massive siltstone, intercalation of bedded sandstone with shales showing turbidite character.	Oligocene
Disang-Barail Transition sequence (Gradational or local tectonic contact) consist of thick siltstone, fine-grained sandstone and sandy or silty shale (Late Eocene –Early Oligocene)		
Disangs	Dark grey splintery shale interbedded with thin siltstone and sandstones showing rhythmites nature.	Late Cretaceous to Late Eocene
<b>~~~~~Unconformity~~~~~</b>		
Basement Complex	Unseen (?) Early Mesozoic/Paleozoic or Precambrian rocks	(?) Early Mesozoic/ Paleozoic

Imphal valley and as outliers in the eastern sides of the valley forming cappings of the Disang Group. Alluvium, which consists of black carbonaceous clay,

standards AGV-2, BCR-2, SCO-1 and multi-element standards were used for calibration, and 10 ppb Rhodium solution was used as an internal standard. To check the accuracy of data, USGS standard BHVO-2, AGV-2 were repeatedly analysed as unknown and the replicate analysis show precision of 2% for the REE, and better than 5% for other elements. Geochemistry data is listed in Tables 2 and 3.

	CH-2	TB-2K-1	TB-W-1	NL-1	NL-3	Ng-3	RTH1
SiO <sub>2</sub>	66.53	72.24	70.90	68.18	72.94	69.05	56.61
TiO <sub>2</sub>	0.58	0.71	0.69	0.40	0.35	0.71	0.81
Al <sub>2</sub> O <sub>3</sub>	10.65	11.44	10.49	12.14	11.05	11.56	19.49
Fe <sub>2</sub> O <sub>3t</sub>	5.74	4.97	4.93	5.15	3.97	5.25	7.61
MnO	0.10	0.06	0.11	0.05	0.05	0.08	0.05
MgO	4.08	2.63	2.87	5.08	4.08	3.24	2.77
CaO	3.19	0.78	1.64	1.01	0.24	1.51	0.48
Na <sub>2</sub> O	2.05	2.53	2.25	3.12	3.50	2.92	0.66
K <sub>2</sub> O	0.67	0.79	0.8	0.53	0.53	0.90	3.15
P <sub>2</sub> O <sub>5</sub>	0.10	0.13	0.12	0.09	0.09	0.14	0.12
L.O.I.	5.93	3.51	4.84	4.18	2.82	4.50	9.42
CIA	51.82	63.97	58.11	61.66	62.07	57.61	78.41
ICV	2.00	1.24	1.53	1.74	1.60	1.54	0.70
PIA	18.74	15.86	16	18.18	16.34	17.77	17.69
MIA	3.65	27.94	16.22	23.32	24.15	15.22	56.81

	CH-2	TB-2K-1	TB-W-1	NL-1	NL-3	Ng-3	RTH1
Sc	11.10	7.76	12.52	10.41	8.99	11.9	16.40
V	71.89	46.98	92	71.08	58.06	91.4	155
Cr	235.8	200.6	548	224.5	254	526	194
Co	14.99	9.77	16.78	19.22	13.3	18.36	22
Ni	32.50	12.05	24.26	42.92	26.90	27.93	205
Cu	24.73	8.02	17.62	16.39	11.48	24.14	49.00
Zn	73.24	30.89	67.99	68.52	48.87	68.37	110
Rb	29.28	23.17	34.91	23.13	15.96	37.96	145
Sr	97.60	52.85	95.92	86.84	142	109	110
Zr	69.90	37.57	114.69	57.79	45.62	96.30	151
Ba	73.4	51.6	89.47	73.66	130	93.36	258
La	30.83	13.59	24.43	13.16	16.66	23.12	29.53
Ce	47.46	24.71	50.18	27.71	35.68	47.71	62.33
Pr	4.59	3.04	6.00	3.23	4.25	5.63	6.83
Nd	17.50	11.48	22.06	13.01	17.02	21.35	29.28
Sm	3.31	2.15	3.88	2.61	3.52	3.87	6.02
Eu	0.74	0.48	0.84	0.65	0.99	0.85	1.36
Gd	3.06	1.92	3.65	2.47	3.67	3.61	4.39
Tb	0.48	0.30	0.52	0.37	0.55	0.60	0.70
Dy	2.73	1.71	3.13	2.36	3.16	3.38	3.88
Ho	0.56	0.35	0.65	0.46	0.63	0.67	0.81
Er	1.64	0.89	1.77	1.26	1.70	1.90	2.49
Tm	0.23	0.15	0.29	0.20	0.26	0.28	0.38
Yb	1.57	0.91	1.77	1.22	1.44	1.77	2.26
Lu	0.22	0.12	0.25	0.17	0.21	0.25	0.36
Ga	4.86	2.70	5.28	5.50	5.35	5.41	24

## RESULTS

### Major and Trace element concentrations

The sandstones are with the high concentrations of Cr (CH-2, Fig. 2 and 3), with CIA value of 51.82 (Table 2). Also, sandstones are high in Al<sub>2</sub>O<sub>3</sub>, K<sub>2</sub>O, V, Ni, Rb and Ba contents (Figs. 2 and 3).

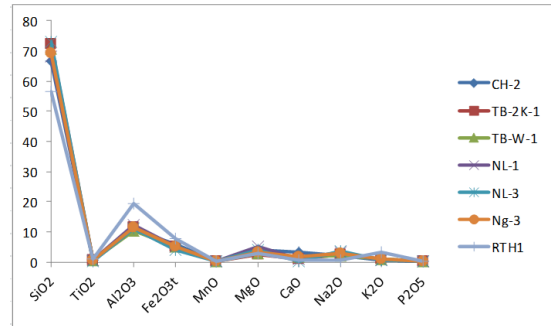


Figure 2. Major element contents in sandstones.

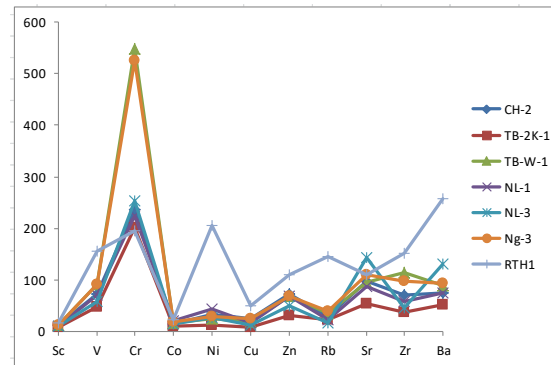


Figure 3. Trace element contents in sandstones.

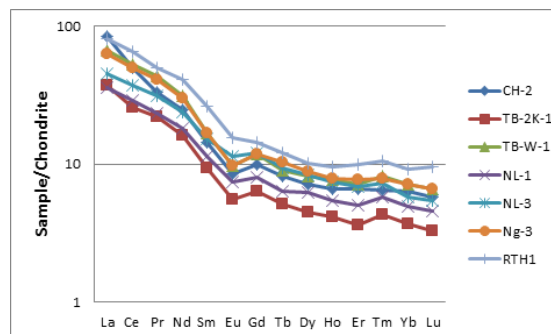


Figure 4. Chondrite normalized diagram for the sandstones from the Imphal Valley.

## MINERALOGY

For mineralogical study, finely powdered samples were mounted in a glass slide and were scanned from 5° to 80° with step size of 0.02° 2θ and with a scan spaced of 10s/step, using nickel filter copper radiation in a Panalytical XpertPro X-Ray diffractometer at the Department of Earth Sciences, Pondicherry University. The mineral phases were identified by using proprietary software Xpert High score.

XRD data (Table 4) show that quartz, albite and clinocllore are the dominant minerals in the studied samples. Clay minerals are kaolinite, vermiculite and montmorillonite (Fig. 5). Albite is mostly related to albitization of feldspars or from low grade metamorphism. Clinocllore occurs as a hydrothermal alteration product of amphiboles,

Sample No.	Minerals
CH-2	Quartz, Clinochlore, albite, Kaolinite
Ng-3	Quartz, Clinochlore, Albite,
TB-W-1	Quartz, Clinochlore, Albite, Montmorillonite
NL-1	Quartz, Clinochlore, Albite, Muscovite
TB-2K-1	Quartz, Albite, Kaolinite, Vermiculite
NL-3	Quartz, Clinochlore, Albite
R-1	Quartz, Clinochlore, Rutile

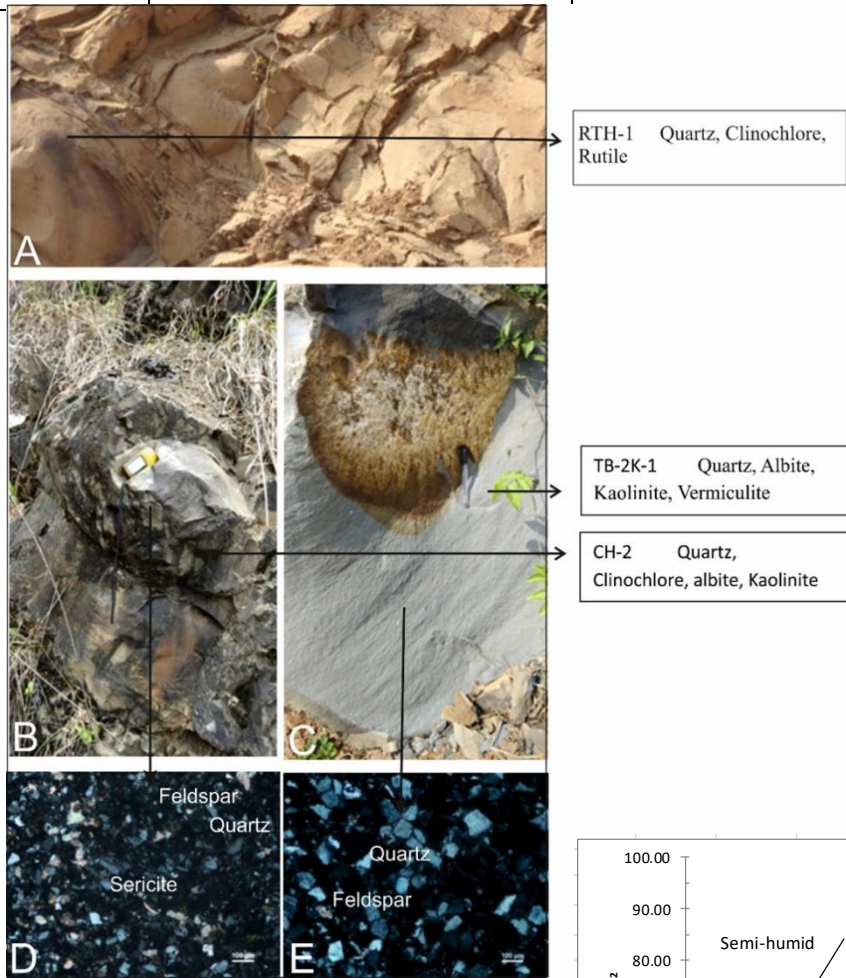


Figure 5. Spheroidal weathering produces rounded boulders within the outcrops (A, B, and C) and photomicrograph of spheroidal weathering (D and E).

pyroxene and biotite. This sediment underwent moderate alteration suitable to clay mineral product as montmorillonite and vermiculite. Alteration of plagioclase allows to form kaolinite. This study suggests the mineralogical composition of the siliciclastic rock of spheroidally weathered from the Imphal Valley. Several primary/secondary mineral pairs can be considered as reflecting the degree of

spheroidally weathering. It is agreed that mineralogy of the incipient stage of rock alteration contained a significant proportion of primary mineral. Albite/montmorillonite are primary/secondary mineral in this study.

### PALEOCLIMATE

Climate and tectonic activity control the alteration of mineral process (Wronkiewicz and Condie, 1987). The high mineral alteration matches the low grade of tectonic and climate fluctuation to hot and moist conditions conducive to mineral degradation in the deposition area (Jacobson and Blum, 2003). The  $SiO_2/(K_2O + Na_2O + Al_2O_3)$  ratio is widely used to discriminate paleoclimate conditions (Suttner and Dutta 1986) because during the alteration phase,  $K_2O$ ,  $Na_2O$  and  $Al_2O_3$  are easily leached compared to  $SiO_2$ .  $SiO_2$  and  $(K_2O + Na_2O + Al_2O_3)$  diagram suggested that the siliciclastic rock from the study area was deposited in the semi-arid climatic conditions (Fig. 6).

Furthermore, the Ga/Rb vs Sr/Cu ratios for the sediments are widely referred to constrain the paleoclimate condition (Xie et al., 2018). Gallium is mostly associated with fine-grained aluminosilicate portion and is high in kaolinite, reflecting hot and moist climate conditions whereas, Rubidium is related with illite and indicates poor intensity of alteration, indicating warm and cool weather conditions (Roy and Roser, 2013a). Therefore, the Ga/Rb value decreases in sediments (Roy and Roser,

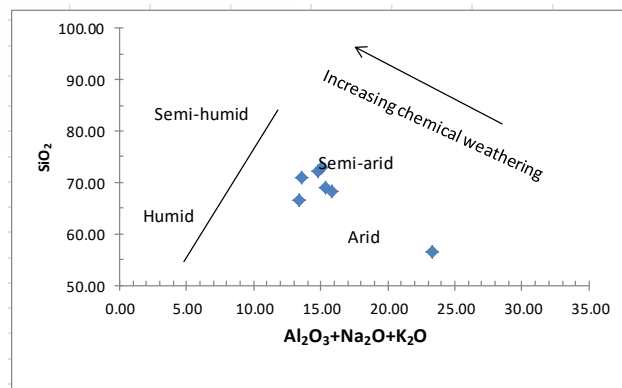


Figure 6 Bivariate plot of  $SiO_2$  vs  $K_2O + Na_2O + Al_2O_3$  to discriminate paleoclimatic conditions (Suttner and Dutta 1986).

2013b) in cold and dry climate conditions, whereas the Ga/Rb value increase in warm and humid climate conditions.

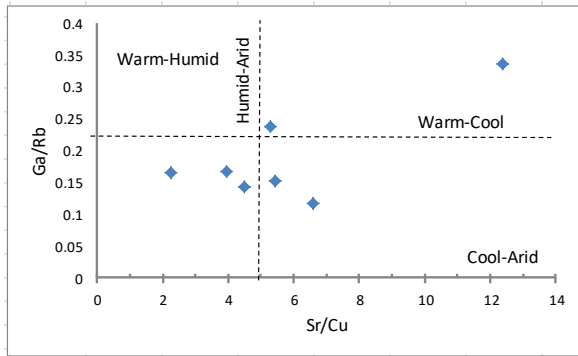


Figure 7. Sr/Cu and Ga/Rb ratios for sandstones from the Imphal Valley (Beckmann et al., 2005; Roy and Roser, 2013 a).

High Ga/Rb and low Sr/Cu proportion value in sediments usually suggest dry and moist weather conditions (Xu et al., 2017). The Sr/Cu proportion value varies between 1.3 and 5.0 in deposits is thought to reveal humid conditions, while values above 5.0 indicate dry conditions (Sarki Yandoka et al., 2015; Xu et al., 2017). The diagram of Ga/Rb and Sr/Cu ratio (Fig. 7) shows low Ga/Rb and Sr/Cu ratio values, which ranges from 2 to 12 for Ga/Rb and 0.1 to .35 for Sr/Cu in most samples. This result reveals the humid-arid and warm cool climate conditions in the source region.

**PALEOWEATHERING and MINERAL**

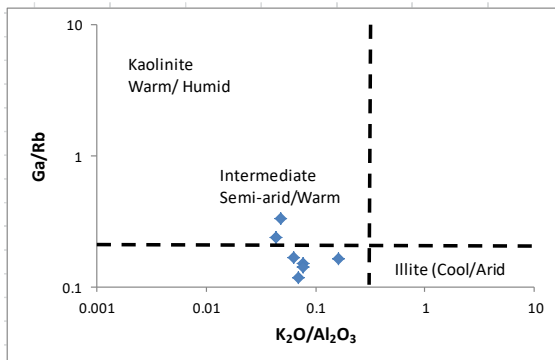


Figure 8. Ga/Rb vs. K<sub>2</sub>O/Al<sub>2</sub>O<sub>3</sub> diagram (Roy and Roser, 2013a).

**ALTERATION**

Chemical weathering influence the chemical composition of the siliciclastic sediments (Nesbitt and Young, 1982, 1984; Johnson et al., 1988; McLennan et al., 1993; Fedo et al., 1995). During this process, Ba and Al are stable in the sediments compared to Ca, Na and Sr that are carried away (Fedo et al., 1996; Nath and Kunzendorf, 2000). According to Nesbitt and Young (1982), the CIA is a good proxy for evaluating sediments alteration and expressed by  $CIA = 100 \times \frac{Al_2O_3}{Al_2O_3 + CaO^* + Na_2O + K_2O}$ . The CIA values are widely used in various studies (Armstrong-Altrin et

al., 2019, 2021a, b; 2022; Ekoa Bessa et al., 2021a, b). The various components are in molar proportions where CaO\* is the quantity of CaO added into silicate fraction of sample. The equation yields values between 50 and 60 for incipient weathering, between 60 and 80 for intermediate weathering, and more than 80 for intense to extreme weathering. In hot and humid tropical condition, sediment have a high CIA value (85-100) and the sediment deposited in the warm humid paleoclimatic have a medium CIA value (70-85) while the lower CIA value (50-70) represents the cold and dry paleo climate, hence, the CIA have been widely used to determine the paleoclimate (Fedo et al., 1995).

The CIA values of this study is varying from 51.82 to 78.41 (Table 2) indicating incipient to intermediate chemical weathering and paleoclimate is varying from cold and dry climate to warm humid climate. The CIA values are integrated into a triangular diagram of Al<sub>2</sub>O<sub>3</sub>-CaO+Na<sub>2</sub>O-K<sub>2</sub>O or A-CN-K (Fig. 9). The siliciclastic rock is close to A-CN axis and suggests a low rate of alteration.

The index of compositional variability ICV >1 is immature and suggests to tectonically active settings (Cox et al., 1995). While those with ICV <1 is mature and deposited in a tectonically stable or cratonic setting, where sediment recycling is active. Accordingly, in this study, the ICV values are >2 with 0.70 of RTH-1 implying that samples are immature and deposited in a tectonically active setting and ICV <1 indicates mature and highly weathered.

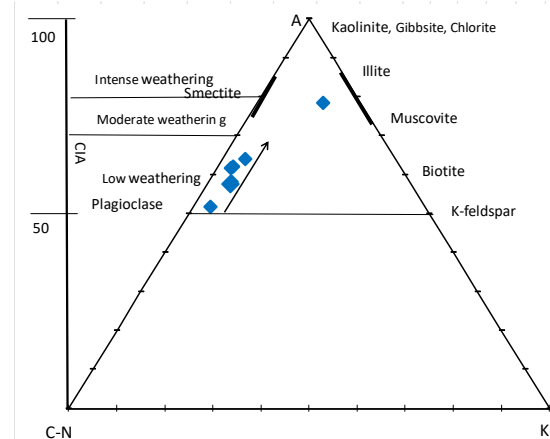


Figure 9 A- CN-K diagram with the CIA values (Nesbitt and Young, 1984)

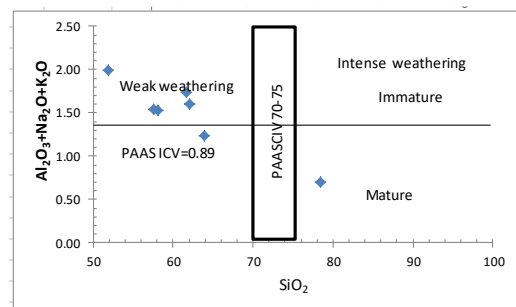


Figure 10. CIA vs ICV binary diagram (Cox et al., 1995; Long et al., 2012).

The binary plot CIA vs ICV (Fig. 10) shows that most of the siliciclastic rocks are geochemically immature and were derived from weakly weathered source rock.

The Plagioclase Index of Alteration (PIA) by Fedo et al. (1995) is used to determine the plagioclase weathering and expressed by  $PIA = \frac{(Al_2O_3 - K_2O)}{(Al_2O_3 + CaO^* + Na_2O - K_2O)} \times 100$  where  $Al_2O_3$ , CaO, NaO and  $K_2O$  are molecular proportions and  $CaO^*$  in the amount of CaO content in the silicate fraction of the rocks. PIA values from 15.7 to 18.7 suggest the incipient weathering of plagioclase. CIA and PIA values for siliciclastic rock show low to moderate silicate weathering (Fig. 11, Roy et al., 2008). The CIA values are in good agreement with those of PIA (Fig. 11).

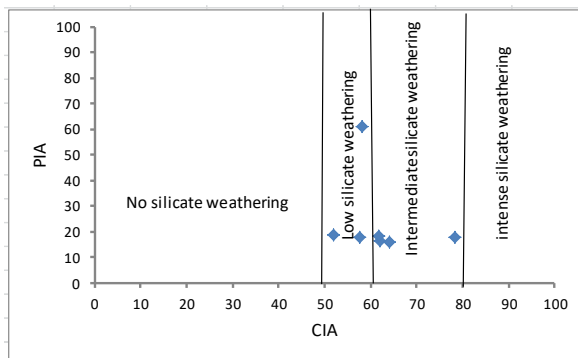


Figure 11. Scatter plots of chemical index of alteration CIA vs. PIA showing the degrees of silicate weathering.

In addition to this, the mineralogical index of alteration (MIA) is used to know the magnitude of the mineralogical weathering of rock formation and is given by

$$MIA = 2X (CIA - 50)$$

The mineralogical index of alteration suggests the degree of mineralogical weathering, i.e. the transformation ratio of a primary mineral into its equivalent alteration mineral. MIA values ranges between 0 and 100, and reflects incipient ( $MIA < 20$ ), intermediate ( $MIA = 20-60$ ), and intense to extreme ( $MIA > 60$ ) mineralogical transformation. The value of 100 means complete transformation of a primary mineral into its equivalent alteration product. The MIA values from 3.65 to 56.81 suggest incipient to intermediate mineral alteration for the sandstones.

### GEOCHEMICAL and MINERALOGICAL VARIATIONS

According to Cullers (2000), Th/Sc ratios near a value of 1.0 are typical of the upper continental crust which tends to be more enriched in the incompatible element Th; whereas, a more mafic component has a ratio near 0.6 and tends to be more enriched in the compatible element Sc (Fig. 12). Intermediately weathered rocks consist more felsic composition.

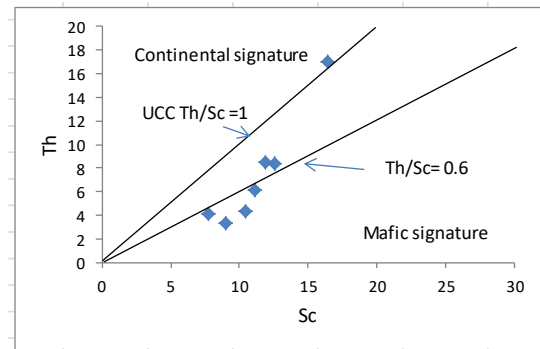


Figure 12. Th vs. Sc plot for the sandstones.

Cr/V-Y/Ni ratios also provide estimates of preferential concentration of chromium over other ferromagnesian elements (Hiscott, 1984; McLennan et al., 1993; Armstrong-Altrin et al., 2014). The Cr/V ratio measures enrichment of Cr with respect to other ferromagnesian elements, whereas the Y/Ni ratio evaluates the relationship between the ferromagnesian trace elements (represented by Ni) and the HREE, using Y as a proxy (McLennan et al., 1993). Y/Ni ratios generally range across values typical of intermediate to felsic calc-alkaline rocks. Sediments derived from ultrabasic sources usually have high Cr/V ratios much greater than 1 coupled with low Y/Ni less than 1 (Hiscott, 1984). The Cr/V ratio for siliciclastic rock is greater than 1.06 and the Y/Ni ratio is less than 1, indicating a contribution of ultramafic rock.

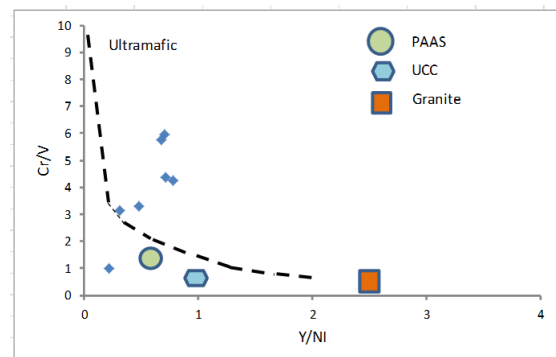


Figure 13 Cr/V vs Y/Ni diagram for the sandstones.

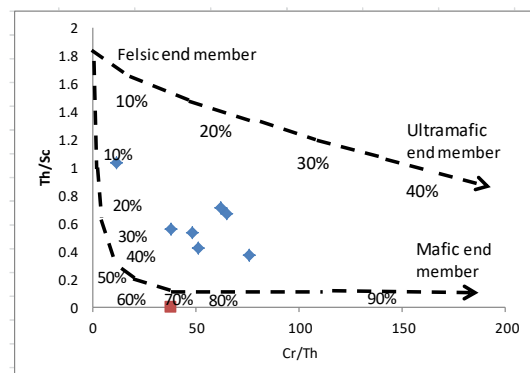


Figure 14. Th/Sc vs Cr/Th ratio in the sandstones (Condie and Wronkiewicz, 1990).

To better constrain the mafic or ultramafic versus felsic character, elemental ratios such as Cr/Th and Th/Sc were considered (Fig. 14). According to Hofmann et al (2003), high values of these ratios reflect enrichment in mafic-ultramafic and felsic components, respectively. The siliciclastic rock indicates a mixing between felsic and mafic end members with a major contribution from the felsic end member for intermediately weathered. This study suggests the geochemical and mineralogical compositions of the weathered rock. Spheroidally weathered originates as a result of expansion during chemical decomposition of the rock.

## CONCLUSIONS

The sandstones from the Imphal valley, Indo-Myanmar Ranges constitute felsic, mafic and ultramafic compositions. Clinocllore suggests hydrothermal alteration of amphibole, pyroxene and biotite. Vermiculite is formed by weathering or hydrothermal alteration of biotite. The rocks were subjected to low – intermediate silicate weathering and low- intermediate mineral alteration. Semi-arid climate condition ranges from humid arid to warm cool prevailed during spheroidal weathering. The moderately weathered rock has dominantly felsic composition than the mafic and ultramafic compositions of less weathered rock. Spheroidal weathered structure originates because of expansion during variations in temperature.

## ACKNOWLEDGEMENTS

The author sincerely thanks the Head, Department of Earth Sciences, Manipur University and Prof. Soibam Ibotombi of the department for providing necessary facilities and support. The author also acknowledged Nurul Absar, Department of Earth Sciences, Pondicherry University and John S. Armstrong-Altrin for geochemical analyses. I thank two reviewers for their useful comments on the manuscript. Author received financial assistance from Department of Science and Technology, New Delhi under the DST project No: SR/WOS-A/EA31/2016 dated 06-01-2017.

## REFERENCES

- Anaya-Gregorio, A., Armstrong-Altrin, J.S., Machain-Castillo, M.L., Montiel-García, P.C., Ramos-Vázquez, M.A. (2018). Textural and geochemical characteristics of late Pleistocene to Holocene fine-grained deep-sea sediment cores (GM6 and GM7), recovered from southwestern Gulf of Mexico. *Journal of Palaeogeography*, v. 7(3), pp. 253-271.
- Armstrong-Altrin, J.S. (2020). Detrital zircon U-Pb geochronology and geochemistry of the Riachuelos and Palma Sola beach sediments, Veracruz State, Gulf of Mexico: a new insight on palaeoenvironment. *Journal of Palaeogeography*, v. 9 (4), article no. 28.
- Armstrong-Altrin, J.S., Nagarajan, R., Lee, Y.I., Kasper-Zubillaga, J.J. and Córdoba-Saldaña, L.P. (2014). Geochemistry of sands along the San Nicolás and San Carlos beaches, Gulf of California, Mexico: implications for provenance and tectonic setting. *Turkish Journal of Earth Sciences*, v. 23 (5), pp. 533-558.
- Armstrong-Altrin, J.S., Botello, A.V., Villanueva, S.F. and Soto, L.A. (2019). Geochemistry of surface sediments from the northwestern Gulf of Mexico: implications for provenance and heavy metal contamination. *Geological Quarterly*, v. 63 (3), pp. 522-538.
- Armstrong-Altrin, J.S., Ramos-Vázquez, M.A., Hermenegildo-Ruiz, N.Y. and Madhavaraju, J. (2021a). Microtexture and U-Pb geochronology of detrital zircon grains in the Chachalacas beach, Veracruz State, Gulf of Mexico. *Geological Journal*, v. 56 (5), pp. 2418-2438.
- Armstrong-Altrin, J.S., Madhavaraju, J., Vega-Bautista, F., Ramos-Vázquez, M.A., Pérez-Alvarado, B.Y., Kasper-Zubillaga, J.J. and Ekoa Bessa, A.Z. (2021b). Mineralogy and geochemistry of Tecolutla and Coatzacoalcos beach sediments, SW Gulf of Mexico. *Applied Geochemistry*, v. 134, pp. 105103.
- Armstrong-Altrin, J.S., Ramos-Vázquez, M.A., Madhavaraju, J., Marca-Castillo, M.E., Machain-Castillo, M.L. and Márquez-García, A.Z. (2022). Geochemistry of marine sediments adjacent to the Los Tuxtlas Volcanic Complex, Gulf of Mexico: Constraints on weathering and provenance. *Applied Geochemistry*, v. 141, pp. 105321.
- Babechuk, Mg., Widdowson, M. and Kamber, Bs. (2014). Quantifying chemical weathering intensity and trace element release from two contrasting basalt profiles, Deccan Traps, India. *Chemical Geology*, v. 363, pp. 56-75.
- Beckmann, B., Fogel, S., Hofmann Schulz, M., and Wagner T. (2005). Orbital forcing of Cretaceous River discharge in tropical Africa and ocean response. *Nature*, v. 437, pp. 241–244.
- Bhatia, M.R. (1983). Rare earth element geochemistry of Australian Paleozoic graywackes and mudrocks: Provenance and tectonic control. *Sedimentary Geology*, v. 45, pp. 97–113.
- Bhatia, M.R. and Crook, K.A.W. (1986). Trace element characteristics of greywackes and tectonic setting discrimination of sedimentary basins. *Contribution to Mineralogical Petrology*, v. 92, pp. 181-193.
- Brantley, S.I., Buss, H., Lebedeva, M., Fletcher, R. and Ma, L. (2011). Investigating the complex interface where bedrock transforms to regolith. *Applied Geochemistry*, v. 26, pp. S12-S15.
- Chabaux, F., Blaes, E., Stille, P., Di Chiara Roupert, R., Pelt, E., Dosseto, A., Ma, L., Buss, H.I. and Brantley, S.I. (2013). Regolith formation rate from U-series nuclides: Implications from the study of a spheroidal weathering profile in the Rio Icaos watershed (Puerto Rico). *Geochimica et Cosmochimica Acta*, v. 100, pp. 73-95.
- Chapman, R.W. and Greenfield, M.A. (1949). Spheroidal weathering of igneous rocks, *American Journal of Science*, v. 247, pp. 407-429.

- Condie, K.C., and Wronkiewicz, D.J. (1990). Cr/Th ratio in Precambrian pelites from the Kaapval craton as an index of craton evolution. *Earth and Planetary Science Letters*, v. 97, pp. 256-267.
- Cox R., Lowe, D.R. and Cullers, R.L. (1995). The influence of sediment recycling and basement composition on evolution of mudrock chemistry in the southwestern United States. *Geochimica et Cosmochimica Acta*, v. 59, pp. 2919-2940.
- Cullers, R.L. (2000) The Geochemistry of Shales, Siltstones and Sandstones of Pennsylvanian-Permian Age, Colorado, USA: Implications for Provenance and Metamorphic Studies. *Lithos*, v. 51, pp. 181-203.
- Devi, S.R. (2021). Geochemistry, depositional and tectonic Setting of the Barail Group of the Indo-Myanmar Ranges. *Journal Indian Association of Sedimentologists*, v. 38, pp. 13-22.
- Devi, S. R. (2022). Geochemistry of the Transitional beds between Disang and Barail Successions of the Imphal Valley, Indo-Myanmar Ranges. *Journal Indian Association of Sedimentologists*, v. 39, pp. 10-16.
- Ehlen, J. (2005). Above the weathering front: contrasting approaches to the study and classification of weathered mantle. *Geomorphology*, v. 67, pp. 7-21.
- Ekoa Bessa, A.Z., Armstrong-Altrin, J.S., Fuh, G.C., Betsi, T.B., Kelepile, T. and Ndjigui, P-D., (2021 a). Mineralogy and geochemistry of the Ngaoundaba Crater Lake sediments, northern Cameroon: implications for provenance and trace metals status. *Acta Geochimica*, v. 40, pp. 718-738.
- Ekoa Bessa, A.Z., Paul-Désiré, N., Fuh, G.C., Armstrong-Altrin, J.S. and Betsi, T.B. (2021b). Mineralogy and geochemistry of the Ossa lake Complex sediments, Southern Cameroon: Implications for paleoweathering and provenance. *Arabian Journal of Geosciences*, v. 14, pp. 322.
- Fedo C.M., Eriksson K.A. and Krogstad E.J. (1996). Geochemistry of shales from the Archean (~ 3.0 Ga) Buhwa Greenstone Belt, Zimbabwe: implications for provenance and source-area weathering. *Geochimica Cosmochimica Acta*. v. 60, pp. 1751-1763.
- Fedo, C.M., Nesbitt, H.W. and Young, G.M. (1995). Unraveling the effects of potassium metasomatism in sedimentary rocks and paleosols, with implications for paleoweathering conditions and provenance. *Geology*, v. 23, pp. 921-924.
- Fletcher, Rc, Buss, H.I. and Brantley, S.I. (2006). A spheroidal weathering model coupling porewater chemistry to soil thicknesses during steady-state denudation. *Earth and Planetary Science Letters*, v. 244, pp. 444-457.
- Hall, K., Thorn, C., and Sumner, P. (2012). On the persistence of weathering. *Geomorphology*, v. 149/150, pp. 1-10.
- Hernández-Hinojosa, V., Montiel-García, P.C., Armstrong-Altrin, J.S., Nagarajan, R., Kasper-Zubillaga, J.J. (2018). Textural and geochemical characteristics of beach sands along the western Gulf of Mexico, Mexico. *Carpathian Journal of Earth and Environmental Sciences*, vol. 13(1), pp. 161-174.
- Hiscott, R.N. (1984). Ophiolitic source rocks for Tectonic-age flysch: trace element evidence. *Geological Society American Bulletin*, v. 95, pp. 1261-1267.
- Hofmann, A., Bolhar, R., Dirks, P.H.G.M. and Jelsma, H.A. (2003). The geochemistry of Archaean shales derived from a mafic volcanic sequence, Belingwe greenstone belt, Zimbabwe: provenance, source area unroofing and submarine vs subaerial weathering. *Geochimica et Cosmochimica Acta*, v. 67, pp. 421-440.
- Jacobson, A.D. and Blum, J.D. (2003). Relationship between mechanical erosion and atmospheric CO<sub>2</sub> consumption in the New Zealand Southern Alps. *Geology*, v. 31, pp. 865-868.
- Johnson, R.W., Perfit M.R., Chappell, B.W. and Jacques A.L. (1988). Volcanism in the New Ireland basin and Manus Island region: notes on the geochemistry and petrology of some dredged volcanic rocks from a rifted-arc region. *Archives*, v. 9, pp. 113.
- Long, X., Sun, M., Yuan, C., Kröner, A. and Hu, A. (2012). Zircon REE patterns and geochemical characteristics of Paleoproterozoic anatectic granite in the northern Tarim Craton, NW China: implications for the reconstruction of the Columbia supercontinent. *Precambrian Research*, v. 222, pp. 474-487.
- McLennan S.M. 1993. Weathering and glacial denudation. *Journal of Geology*, v. 101, pp 295-303.
- McLennan, S.M., Hemming, S., McDaniel, D.K. and Hanson, G.N. (1993). Geochemical approaches to sedimentation, provenance, and tectonics. *Johnsson M.J., Basu A., editors. Processes controlling the composition of clastic sediments. Geological Society of America Special Paper*, v. 284, pp. 21-40.
- Nath B.N. and Kunzendorf H. (2000). Influence of provenance, weathering, and sedimentary processes on the elemental ratios of the fine-grained fraction of the bedload sediments from the Vembanad, Lake and the Adjoining Continental Shelf, Southwest Coast of India. *Journal of Sedimentary Research*, v. 70(5), pp. 1081-1094.
- Nesbitt H.W. and Young G.M. (1982). Early Proterozoic climates and plate motions inferred from major elements chemistry of lutites. *Nature*, v. 199, pp. 715-717.
- Nesbitt H.W., Young G.M. 1984. Prediction of some weathering trends of plutonic and volcanic rocks based on thermodynamic and kinetic considerations. *Geochimica et Cosmochimica Acta*. v. 48, pp. 1523-1534.
- Ollier, C.D. (1971). Causes of spheroidal weathering, *Earth-Sciences Reviews*, v. 7, pp. 127-141.
- Roser, B.P. and Korsch, R.J. (1986). Determination of tectonic setting of sandstone-mudstone suites using SiO<sub>2</sub> content and K<sub>2</sub>O/Na<sub>2</sub>O ratio. *The Journal of Geology*, v. 94, pp. 635-650.
- Roy D.K. and Roser B.P. (2013a). Climatic control on the composition of carboniferous-Permian Gondwana



- sediments, Khalaspir, Bangladesh. *Gondwana Research*, v. 23, pp. 1163-1171.
- Roy D.K. and Roser B.P. (2013b). Geochemical evolution of the Tertiary succession of the NW shelf, Bengal basin, Bangladesh: Implications for provenance, paleoweathering and Himalayan erosion. *Journal of Asian Earth Sciences*, v. 78:248–262.
- Roy, P.D., M. Caballeroa, R. Lozanoc and W. Smykatz-Klossd (2008). Geochemistry of late quaternary sediments from Tecocomulco Lake, central Mexico: Implication to chemical weathering and provenance. *Chemie der Erde*, v. 68, pp. 383-393.
- Sarki Yandoka B.M., Abdullah W.H., Abubakar M.B., Hakimi M.H. and Adegoke A.K. (2015). Geochemical characterization of Early Cretaceous lacustrine sediments of Bima Formation, Yola Sub-basin, Northern Benue Trough, NE Nigeria: Organic matter input, preservation, paleoenvironment and palaeoclimatic conditions. *Marine and Petroleum Geology*, v. 61, pp. 82-94.
- Soibam, I. (1997). Structural control on ground water occurrence in shales: a case study of the Imphal valley. *Indian Journal of Landscape Systems and Ecological Studies*, v. 20, pp. 111-116.
- Sopie, F.T., Ngueutchoua, G., Armstrong-Altrin, J.S., Njanko, T., Sonfack, A.N., Sonfack, A.N., Ngagoum, Y.S.K., Fossa, D. and Tembu, L.T. (2023). Provenance, weathering, and tectonic setting of the Yoyo, Kribi, and Campo beach sediments in the southern Gulf of Guinea, SW Cameroon. *Journal of Earth System Science*, 132, article no. 92.
- Stallard Rf. (1995). Tectonic, environmental, and human aspects of weathering and erosion: A global review using steady-state perspective. *Annual Review Earth and Planetary Sciences*, v. 23, pp. 11-39.
- Suttner L. and Dutta P. (1986). Alluvial sandstone composition and paleoclimate. I. Framework mineralogy. *Journal of Sediments*, v. 56, pp. 329-345.
- Turkington Av, Phillips Jd and Campbell, Sw. (2005). Weathering and landscape evolution. *Geomorphology*, v. 67, pp. 1-6.
- Wronkiewicz D.J. and Condie K.C. (1987). Geochemistry of Archean shales from the Witwatersrand Supergroup, South Africa: source-area weathering and provenance. *Geochemica Cosmochimica Acta*, v. 51, pp. 2401-2416.
- Xie G., Shenc Y., Liuab S. and Haod W. (2018). Trace and rare earth element (REE) characteristics of mudstones from Eocene Pinghu Formation and Oligocene Huagang Formation in Xihu Sag, East China Sea Basin: Implications for provenance, depositional conditions and paleoclimate. *Marine and Petroleum Geology*, v. 92, pp. 20-36.
- Xu, Q.L., Liu, B., Ma, Y.S., Song, X.M., Wang, Y.J. and Chen Z.X. (2017). Geological and geochemical characterization of lacustrine shale: A case study of the Jurassic Da'anzhai member shale in the central Sichuan Basin, southwest china. *Journal of Natural Gas Science*, v. 47, pp 124-139.

*Received on: April 6, 2024*

*Revised accepted on: Oct 7, 2024*